Multidisciplinary Experimental Approaches to Characterizing Biomolecular Dynamics

Floyd E. Romesberg*[a]

KEYWORDS:

3PEPS · laser spectroscopy · molecular recognition · protein dynamics · tautomerism

1. Introduction

The molecules that make life possible, in particular proteins and nucleic acids, have evolved over billions of years to possess the properties that enable them to perform specific functions. As products of the evolutionary process, these molecules are very different from abiological molecules—*biological molecules have, in a sense, learned how to perform specific functions*. Biological molecules may have evolved structure–function relationships that are entirely unlike abiological molecules, whose characteristics in this sense are more random. For example, there is an increasing amount of experimental data that has been interpreted in terms of specific protein motions that facilitate catalysis by coupling to the substrate reaction coordinate.[1–4] At present, molecular dynamics (MD) simulations of enzymatic reactions have found no direct evidence of dynamical effects in catalysis,[5–7] although several theoretical studies have supported such an interpretation.[8, 9] In order to test these hypotheses experimentally, detailed structural and dynamic information is required. While impressive advances have been made in the structural characterization of biomolecules, their dynamic characterization has remained a challenge because their inherent complexity has precluded the use of many conventional techniques.

By combining recent advances in technology and a multidisciplinary approach that draws on the tools of organic synthesis, physical methods, and molecular biology, innovative techniques to facilitate the dynamic characterization of biomolecules may be developed. We have developed three systems to study DNA and protein dynamics, which are described in this review. The first is a model base pair to probe tautomerization dynamics in nucleic acids; the second is a technique based on deuterium isotope substitution in proteins that allows for the observation of specific protein vibrations; and the third is a femtosecond multipulse laser experiment to examine protein flexibility.

2. A Phototautomerizable Model Base Pair to Probe the Environment and Dynamics of Duplex DNA

DNA is virtually always discussed in terms of base pairs between keto–amine tautomers, although each pair may be converted to its enol–imine form by double proton transfer (prototropic tautomerism, Scheme 1 a). It is not known how the relative stability of the tautomers is affected by the environment, which includes factors such as packing interactions with flanking bases

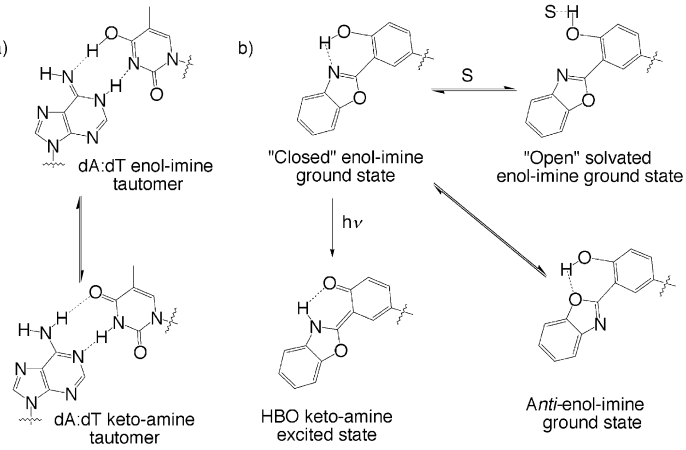

Scheme 1. *a) Prototropic tautomerization in a natural dA:dT base pair. b) Equilibrium of HBO ground states and photoinduced tautomerization.*

and the influence of waters of solvation available in the major and minor grooves. Proteins that bind DNA may also influence the stability of the tautomers. Tautomerization in turn may influence the physical and dynamic properties of DNA, such as duplex flexibility, protein recognition, or polymerase-mediated replication, by providing dipolar coupling between flanking base pairs. Unfortunately, the proton transfer process that interconverts the tautomers has been difficult to study because of its fast timescale, minimal heavy atom motion, and inherent reversibility. In addition, tautomerization cannot be initiated within a specific dA:dT or dG:dC base pair in a duplex DNA molecule.

[a] *Prof. F. E. Romesberg*
Department of Chemistry
The Scripps Research Institute
10550 North Torrey Pines Road Maildrop CVN22
La Jolla CA 92037 (USA)
Fax: (+1) 858-784-7472
E-mail: floyd@scripps.edu

 DOI: 10.1002/cbic.200300572

A model to study base-pair tautomerization has been based on the double proton transfer of 7-azaindole dimers.[10–13] Experiments have been directed at understanding the proton transfer dynamics as well as how this process is influenced by solvation and heteroatom substitution. For example, in hydrocarbon solvents, fluorescence upconversion experiments show a 1-ps decay in the 360-nm dimer emission, which has been associated with proton transfer. This timescale was also observed as a rise time of the tautomer emission at 480 nm. A longer component (12-ps time constant) was also observed at 480 nm and was assigned to an excited-state relaxation process, which may be related to solvation dynamics.[10] The addition of strongly hydrogen-bonding solvents such as water or an alcohol results in solvated monomers in which proton transfer is either blocked or occurs through solvent assistance.[14] Purine-like nitrogen substitution of the indole ring was found to selectively destabilize the excited tautomer and thus increase the barrier to proton transfer.[15] While these studies have elegantly elucidated the tautomerization dynamics of an isolated base pair model, DNA base pairs exist in the duplex environment, which may have evolved to influence tautomerization.

In order to study tautomerization at a defined position within duplex DNA, we developed 2-(2′-hydroxyphenyl)benzoxazole (HBO) as a model DNA base pair (Scheme 1).[16–19] Tautomerization of HBO may be selectively and efficiently initiated when photoexcitation at 333 nm induces excited-state intramolecular proton transfer (ESIPT). One major advantage of HBO as a model DNA base pair is that, unlike other common models such as 7-azaindole,[12, 15, 20] HBO may be incorporated into and induced to tautomerize in duplex DNA, thus providing a probe of tautomerization in the environment of a natural base pair. The nucleoside with HBO attached through a *C*5′-aryl-glycosidic linkage (Scheme 1) was synthesized and converted into the corresponding phosphoramidite. The phosphoramidite was incorporated in the oligonucleotide 5′-CGTTTC(HBO)TTCTC by using automated DNA synthesis. This single-stranded DNA was annealed to a complementary oligonucleotide containing an abasic site at the position opposite HBO. Both the CD and UV/Vis spectra were consistent with a well-packed A-form duplex. The duplex was virtually as stable to thermal denaturation as the corresponding duplex with a dA:dT base pair (melting temperatures, $T_m = 38$ and 39 °C, respectively). The accommodation of the model base pair within a native-like duplex was also supported by molecular dynamics simulations, which indicated that HBO packs within duplex DNA with the phototautomerizable O–H···N bond disposed in the major groove (Figure 1).

The dynamic behavior of HBO may be understood by first considering the conformational equilibrium between the *syn*- and *anti*-enol conformers, with either an intramolecular hydrogen bond ("closed") or an intermolecular hydrogen bond with a solvent molecule ("solvated"), as depicted in Scheme 1. ESIPT is only possible in the closed *syn*-enol, which yields the excited keto form and gives rise to a strongly red-shifted emission band at around 500 nm. ESIPT is not possible with a solvated enol because of disruption of the hydrogen bond, nor with the *anti* form because of an insufficient increase in the pK_a value of the benzoxazole oxygen atom upon excitation.

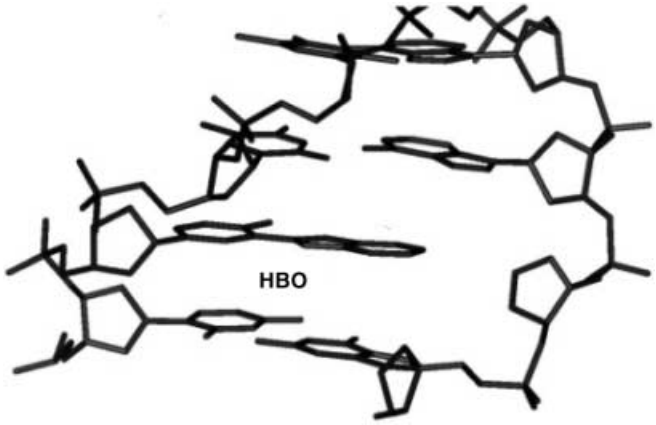

Figure 1. *Simulated structure of HBO in DNA duplex.*

In the DNA duplex sequence examined, HBO exists virtually exclusively in the closed *syn*-enol conformer, based on the 338-nm absorption maximum and a single, strongly Stokes-shifted fluorescence band at 480 nm. In single-stranded DNA (ssDNA), the steady-state emission spectrum of HBO is qualitatively different. In addition to emission at 485 nm, a strong fluorescence band was observed at 370 nm, indicative of a significant concentration of the solvated or closed *anti*-enol ground states.[21–25] The different conformational equilibrium of HBO in duplex, as compared to ssDNA, is supported by excitation-dependent fluorescence spectra.[17] Duplex formation precludes HBO solvation and strongly favors the closed *syn*-enol form of the model base pair.

After excitation, ESIPT converts the *syn*-enol to the excited keto tautomer. Thus, there are at least two components to HBO tautomerization: proton transfer dynamics and keto dynamics. Fluorescence upconversion was used to measure the excited state proton transfer time, which was found to be 150 fs in both single-stranded and duplex DNA,[19] and approximately 170 fs for free HBO in hexane, methanol, and dimethyl sulfoxide.[18] The invariance of the rate implies that the proton transfer within the model base pair is not strongly influenced by the environment. The fluorescence lifetime of the excited keto tautomer was measured by transient absorption and time-resolved fluorescence spectroscopies.[17, 18] For free HBO, the keto lifetime was found to increase with solvent polarity. The fluorescence decay of the excited keto tautomer in duplex DNA and in ssDNA were indistinguishable ($2.0 \times 10^8\ s^{-1}$), but 17-fold slower than in hexane. The internal duplex environment appears to be more dipolar than dimethyl sulfoxide, despite the exclusion of water molecules.

While the duplex environment does not affect the rate of proton transfer, as might have been expected considering the strongly adiabatic nature of ESIPT, the environment does appear to strongly influence the solvation, conformation, and tautomer stability of the model base pair. It appears that the model base pair is not solvated by water molecules readily available in the major groove. This is not a property inherent to HBO, as the internal hydrogen bond is disrupted by hydrogen-bonding solvents such as methanol and by water when HBO is

incorporated in ssDNA.[18] After sequestering the model base pair from solvation, the flanking base pairs appear to establish a strongly polar but anisotropic environment that selectively stabilizes the *syn*-enol tautomer of the model base pair in the ground state and the keto tautomer in the excited state. The duplex environment strongly favors nitrogen protonation and increased double-bond character of the hydroxyphenyl C—O bond, that is, the keto – amine-like tautomer of HBO. The duplex environment may have evolved to favor the keto – amine tautomers of natural base pairs, whose dominance is critical for DNA function, including replication. To further probe the environment and dynamics of DNA, HBO is currently being incorporated into DNA through a *C*3′-glycosidic linkage (at the position *ortho* to the phenolic oxygen atom). In this context, the model base pair should allow study of tautomerization in the duplex minor groove.

3. A Novel Probe of Protein Dynamics: Selective Incorporation of C—D Bonds

The most fundamental way to understand any molecule is to characterize the nature of the bonds that give the molecule its particular shape, stability, and flexibility (i.e., define the molecule's potential energy surface). Of course, any chemical bond, including those of biomolecules such as proteins may be characterized by IR spectroscopy. Spectral congestion inherent to proteins from the many overlapping IR absorptions has prevented the use of the conventional spectroscopic methods employed to characterize small molecules.

Attempts to circumvent the spectral complexity problem have focused on using isotopic labeling, in conjunction with difference Fourier transform infrared (FTIR) spectroscopy, to observe specific protein absorptions, for example, in the amide region of the IR spectrum (around 1700 cm^{-1})[26, 27] The amide I band has proven most useful. The amide I band arises from the C=O stretching vibrations, with smaller and structure-dependent contributions from the out-of-phase C—N stretching as well as C—C—N and C—N—H bending vibrations.[28–30] The structure-dependent composition of the band along with structure-dependent coupling of the transition dipole moments and hydrogen bonding, make the amide I band, including the absorption frequency, linewidth, and intensity, sensitive to the peptide conformation. For example, temperature-induced decreases in intensity and shift of amide I vibrations at the C terminus of helical peptides have been interpreted in terms of end fraying[31] and localized conformational changes.[32] In addition, the amide I band linewidth contains interesting information about the flexibility of the peptide or protein (the inherently short timescale of IR vibrations (10^{-13} s) makes them particularly informative in this regard). The amide I absorption frequency is a sensitive function of the environment, therefore the multiple environments that result from more flexibility lead to line broadening. This broadening has been used to characterize flexibility changes that might contribute to catalysis[33] and protein binding.[34–41] These studies remain challenging, and are largely focused on model peptides because of spectral congestion and the inherent difficulties in the analysis of difference spectra where very large protein absorptions must be precisely cancelled to reveal the much less intense absorption that is due to a single or a few protein vibrations.

An interesting feature of all proteins is that there is a 'transparent window', between 1800 and 2700 cm^{-1}, which is free of absorptions (Figure 2). Any bond vibrations that absorb in this region are directly observable without spectral subtraction, even at high protein and denaturant concentrations. Previous

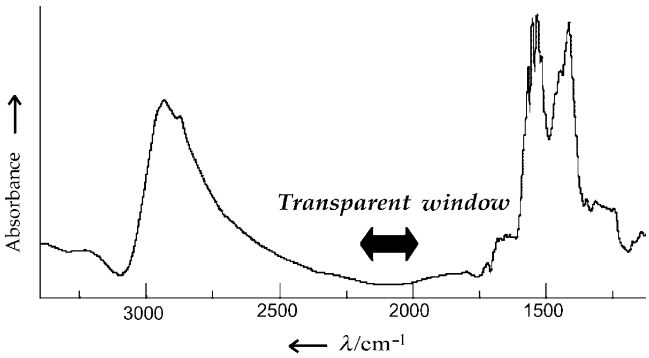

Figure 2. *Transparent window in the protein FTIR spectrum.*

experiments have taken advantage of this window to observe the stretching vibrations of small molecules bound to heme proteins, such as carbon monoxide (≈1950 – 2150 cm^{-1}) in myoglobin,[42–47] hemoglobin,[48, 49] and guanylate cyclase,[50] or azide (≈2050 cm^{-1}) in cytochrome bo_3.[51] In these studies, the absorption frequency and linewidth of the ligand bond are used to (indirectly) characterize the protein environment and dynamics. Though informative, these small molecule probes do not report directly on the protein.

Characterization of protein dynamics would ideally utilize direct probes of the protein that also absorb in the 'transparent window' of the protein IR spectrum. Carbon – deuterium (C—D) bonds are such probes. The C—D bond absorbs within the transparent window at around 2100 cm^{-1} and provides a local-mode vibration whose absorption frequency may be interpreted in terms of bond strength (force constant) and environmental polarity, and whose linewidth may be interpreted in terms of protein flexibility (since inhomogeneous broadening results from an increased sampling of different environments in the more flexible proteins).[52] These properties of the C—D stretching frequency and linewidth have been used previously to characterize small-molecule structure and dynamics[53–63] and we have recently expanded their application to include proteins.[64, 65]

To develop the method, we focused our initial efforts on horse heart cytochrome *c* (cyt *c*). Cyt *c* functions as an electron carrier in the mitochondrial electron-transport chain by using the Fe^{II} – Fe^{III} redox couple of a covalently attached heme prosthetic group that is ligated by His18 and Met80. The Fe—S bond between the heme group and the protein-based Met80 ligand is thought to play a critical role in the function and folding of the protein. Therefore, we were interested in examining the environment and dynamics of this ligand.

Selective deuteration of the methyl group of Met80 in horse heart cyt *c* was performed by means of bacterial expression in defined minimal media supplemented with the deuterated amino acid, and resulted in easily observable C—D absorption bands (Figure 3).[64, 65] The Met80 methyl group vibrations seem

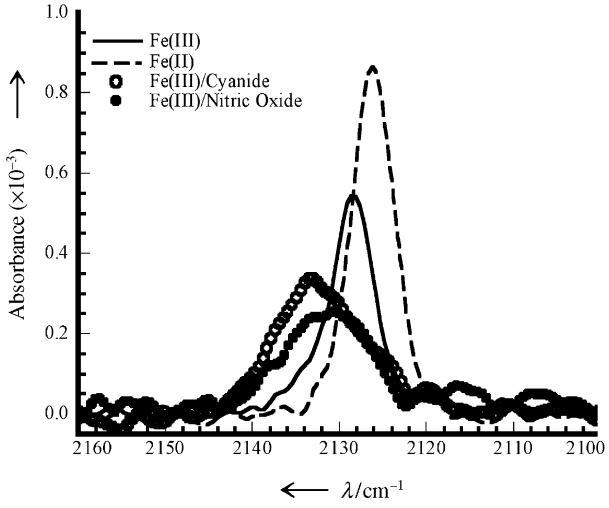

Figure 3. *C—D absorption of (methyl-d_3)methionine-labeled M65L cytochrome c: oxidized, pH 5 (solid line); reduced with ascorbic acid (dashed line); oxidized with Met80 displaced from the heme Fe atom by the addition of $K^{13}C^{15}N$ (open circles); oxidized with Met80 displaced from the heme Fe atom by the addition of nitric oxide (closed circles).*

to be most sensitive to the vicinal Fe—S bond. The methyl group vibrations become stronger (shift to higher frequency) upon cleavage of the Fe—S bond with isostructural but differently charged ligands (CN^- and NO), and become weaker (shift to lower frequency) upon strengthening of the Fe—S bond by reduction.[65] These data imply that these specific protein vibrations are primarily sensitive to through-bond hyperconjugative interactions with sulfur-based orbitals and not the overall electrostatic field at Met80. It is interesting to compare this model to the model developed to explain the CO stretching frequencies in carbonmonoxycytochrome *c*, in which polar interactions are thought to be most important and act by increasing or decreasing $Fe_{d\pi} - CO_{\pi^*}$ backbonding.[66] The orbitals involved in π backbonding are more polarizable than those involved in covalent or hydrogen-bonding interactions. To manipulate these critical, but less polarizable bonds, proteins may have had to evolve more direct 'through-bond' interactions.

In a second study of Met80,[64] we investigated the relationship between ligand motion and redox potential. Proteins with systematically altered redox potentials were generated by mutation at Phe82. The aromatic portion of this side chain packs on the heme cofactor while the methylene unit is in van der Waals contact with the Met80 methyl group. Crystal structures of iso-1-cyt *c* with Phe82 mutated to Gly, Ser, and Tyr have shown that this residue tolerates a wide variety of substitutions with only local structural readjustments,[67, 68] and in vivo studies have demonstrated that the protein will fold and function with any of the twenty amino acids at this position.[69] However, in vitro, Phe82 mutation has been found to have a large effect on the redox potential of the protein, possibly as a result of changes in binding-site hydrophobicity, solvent or substrate accessibility, or protein dynamics. We examined the stretching frequency and linewidth of the deuterated Met80 ligand in six mutant proteins in which Phe82 was exchanged for His, Ser, Leu, Val, Ala, and Gly. The redox potential was also determined for each mutant.

Like the wild-type (wt) protein, the oxidized state of each mutant protein exhibited a stronger C—D bond than the reduced state, as indicated by the higher C—D stretching frequency of each oxidized protein (Figure 4a). There is only a weak

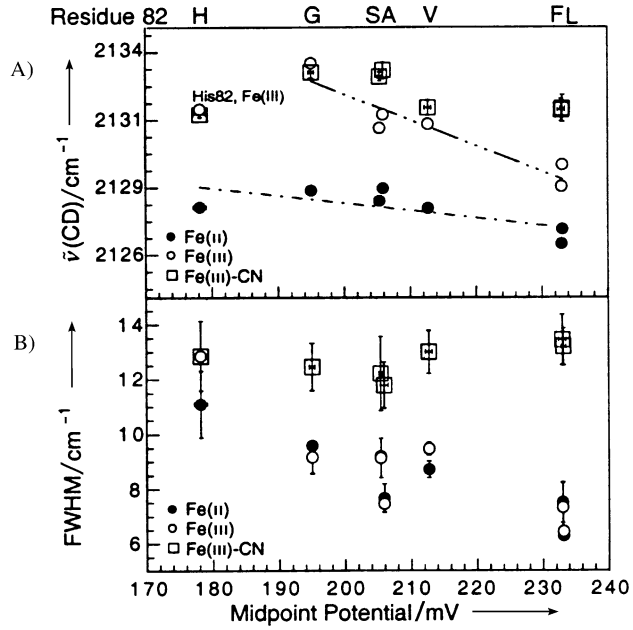

Figure 4. *Redox dependence of (A) the C—D stretching frequency and (B) the C—D linewidth (FWHM, full width at half maximum) of (d_3-methyl)Met80 in wt and Phe82 mutants of cyt c. Linear correlations are shown for the $\tilde{\nu}$(CD) values of the reduced and oxidized fit. The identity of residue 82 is indicated at the top of the figure.*

correlation between C—D bond strength and redox potential, which implies that there are no major changes in the local polarity of the Met80 ligand accompanying oxidation or reduction. However, when the C—D linewidth is plotted as a function of the redox potential (Figure 4b), a strong correlation is observed that relies on an intact Fe—Met80 bond. The methyl group vibrations are apparently sensitive to a mutation-dependent broadening mechanism, but only when Met80 is ligated to the metal center. Such broadening in the condensed phase is primarily due to environmental heterogeneity, where the C—D bond is sensitive to, and experiences, multiple environments. While this does not affect the average frequency (in agreement with the data described above), it does broaden the absorption line. Thus, mutation at Phe82, which generally causes a reduction in the redox potential of the protein (that is, stabilizes the Fe^{III} state relative to the Fe^{II} state), appears to be correlated with increased protein flexibility at Met80.

Despite the sensitivity of ligand motion to redox potential, the linewidths of Met80 C—D absorptions are identical in the oxidized and reduced states (Figure 4b). The oxidation-state independence of the observed linewidths is of particular interest because oxidation-state-dependent changes in protein flexibility have often been invoked to explain the distinct behaviors of the protein in the two oxidation states.[70, 71] The linewidth data rule out any redox-dependent changes in the motions of the protein, at least at the Met80 ligand. Apparently, mutation of the protein at position 82 causes a redox-state-independent increase in the fluctionality of the protein. The more flexible protein may favor the more polar oxidized state by allowing increased transient water penetration[72–74] or by allowing subtle protein reorientation.[75, 76] In either case, cyt *c* may have evolved to maximize structural rigidity in order to provide the hydrophobic environment required to tune the Fe^{II} – Fe^{III} redox couple appropriately for biological function.

A particularly powerful aspect of this method is the ability to selectively observe vibrations associated with any part of the protein. In order to realize this potential we have generated cyt *c* semisynthetically.[77] We site-selectively incorporated CδCγ-d_4 deuterated lysine (residue Lys88), Cδ-d_3 deuterated leucine (at residues Leu68, Leu94, and Leu98), and Cβ-d_3 deuterated alanine (at residues Ala83, Ala96, and Ala101). The stretching absorptions are readily apparent in each case. Generally, the frequency and linewidth of the observed vibration depend on the part of the protein being probed, and in some cases on the redox environment. A complete characterization of these deuterated proteins, as well as of those with C—D bonds incorporated elsewhere, should begin to develop a complete picture of the local environment and flexibility of cyt *c* with residue-specific detail.

We have also determined that C—D bonds incorporated throughout cyt *c* are sensitive to the folded state of the protein.[77] The spectral first moments (that is, average absorption frequency) show dramatic two-state transitions upon titration of the protein solution with denaturant. Importantly, the transition midpoints associated with C—D bonds incorporated at different positions of the protein are not the same, which demonstrates that cyt *c* unfolds in a stepwise manner as the denaturant concentration is increased. Thus, a residue-specific view of the folding process is possible with this technique. We note that the method is applicable to proteins in general, and C—D bonds have been incorporated into dihydrofolate reductase, myoglobin, and hemoglobin, and in each case the C—D bonds are easily observed.[77]

4. Use of Ultrafast Multiple-Pulse Spectroscopy to Characterize Protein Flexibility

Protein flexibility is likely to play an important role in molecular recognition by allowing optimization of the protein – ligand or protein – protein binding interactions. The amount of optimization required may range from little, that is, the 'lock-and-key' model,[78] to extensive, that is, the 'induced fit' model.[79] These two limiting models of molecular recognition are differentiated only by the role of flexibility. To address these models experimentally, it is critical to characterize protein flexibility. Since antibodies (Ab) represent the most successful example of molecular recognition known, a study of Ab flexibility may prove to be particularly informative.

In order to study how Ab recognize their target antigens (Ag), they have been structurally characterized, both free and with bound Ag, in order to detect any conformational changes associated with Ag binding. A variety of structural rearrangements have been documented, which range from small (consistent with induced fit) to large (consistent with lock-and-key) structural changes.[80–89] However, the protein flexibility that is central to differentiating between the models of molecular recognition is not necessarily manifest as differences between average structures, nor necessarily in the average fluctuation about the average structure. More direct evidence of flexibility has been collected by characterizing the binding kinetics by using stopped-flow fluorescence experiments. In most cases, the binding kinetics are single exponential relationships, and thus do not require Ab conformational changes to be considered. However, multiexponential kinetics have been observed for the binding of 2-phenyl-5-oxazalone[90] and 2,4-dinitrophenyl[91] to their respective Ab. In addition, structural studies showed that 2-phenyl-5-oxazalone binding induced an Ab conformation that was different from that induced by a protein Ag that also binds the same Ab.

In order to more quantitatively address the mechanism of Ab-based molecular recognition, flexibility must be carefully defined. A simple and intuitive view of the flexibility of any material, including an Ab, is based on its response to an applied force.[92–94] For example, a flexible Ab will respond to a given force with large amplitude, low frequency motions, while a more rigid protein will respond to a similar force with smaller amplitude, higher frequency motions. A step-function force may be applied to the antigen (Ag) binding site of an Ab by electronic excitation if the Ag is also a chromophore. Excitation induces changes in both Ag electron density and structure and produces an Ab – Ag complex that is out of equilibrium. The Ab will be subjected to a force until protein motions re-establish equilibrium with the excited chromophore. The frequency distribution of these motions may be determined from femtosecond three-pulse photon echo peak shift (3PEPS) spectroscopy[95–97] and expressed as a spectral density, $\rho(\omega)$, which describes the amplitude of fluctuations as a function of frequency (ω).

The 3PEPS experiment is similar to the well-known NMR spin echo experiment, but requires three pulses of light resonant with the chromophore absorption (Figure 5). In brief, the first pulse initiates the first time period (τ), during which time the system is in an electronic superposition state of the ground and excited states. During this period, the ensemble begins to dephase because of the slightly different environments of each chromophore (each chromophore of the ensemble experiences a binding site that at any instant is unique). The second pulse initiates the second time period (T), during which the system is in a population state, where no dephasing is possible. The third pulse places the system back in a coherence state and initiates a rephasing of the nonlinear polarization, which results in a

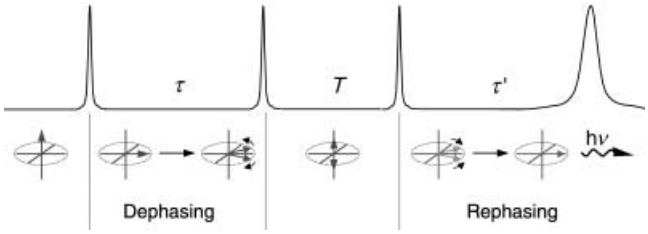

Figure 5. *A 3PEPS experiment and the vector model description of electronic dephasing during τ and rephasing during τ'.*

macroscopic dipole and the emission of a photon (the photon echo). The ability to vary *T* is critical to allow the dephasing to be 'effectively frozen' while the dynamics of the protein continue to evolve. When *T* is short (compared to the timescales of protein dynamics), rephasing occurs in the same environment as dephasing, which results in complete rephasing and a maximal echo signal. However, when *T* is long compared to the timescales of protein dynamics, the environment changes between the dephasing and rephasing periods, which results in incomplete rephasing and a decreased echo signal. The echo intensity thus decays as a function of *T*, in a manner that depends on the protein vibrations that act to randomize the environment. The echo intensity is measured by integrating over the final time period as a function of *T*. The experimentally observable decay of the photon echo peak shift (the location in time of the echo maximum, τ') is known to reflect the timescales and amplitudes of $M(t)$, the time domain representation of $\rho(\omega)$.[95]

To apply this methodology, we characterized two sets of Ab that each bind one of the chromophoric Ag 8-methoxypyrene-1,3,6-trisulfonate (MPTS) or fluorescein (Fl).[97, 98] Ab were specifically elicited for each Ag in mice by using standard monoclonal

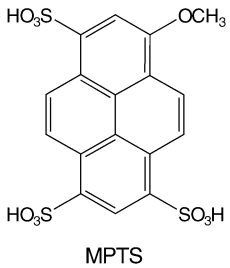

MPTS

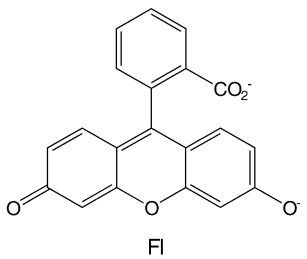

Fl

technology. The Ab were cloned and sequenced as reported previously.[97, 98] One anti-MPTS and three different anti-Fl Ab were extensively characterized. The spectral densities were determined for each Ab by 3PEPS spectroscopy as described previously.[97, 98]

Characterization of an anti-MPTS Ab, 6C8, by 3PEPS revealed that MPTS excitation induced three protein motions.[97] A large-amplitude, ultrafast protein motion was observed that accounts for 71% of the protein reorganization energy (the decrease in energy associated with the Ab motions which act to re-establish equilibrium with the excited Ag) on a 75-fs timescale. Two slower Ab motions with timescales of 2 ps and 67.4 ps were also observed, which account for 18% and 11% of the combining site reorganization energy, respectively.

Ab combining sites are comprised of six complementarity determining region (CDR) loops, three from the light chain (LC CDR 1 – 3) and three from the heavy chain (HC CDR 1 – 3). The majority of Ab – Ag contacts are typically provided by the two CDR3s. The ultrafast response may be inertial and may result from nearly free motion of a polarizable side chain within these two loops. Candidate amino acids include methionine and phenylalanine, which have the only polarizable side chains that are expected to be sufficiently mobile. In both the light- and heavy-chain CDR3 loops, 6C8 has a single phenylalanine residue, PheH100,[99] and no methionine residues. Thus, it is possible that motion of PheH100 contributes to the 6C8 combining site reorganization. Interestingly, structural studies of other Ab have shown that aromatic residues at similar positions of the HC CDR3 undergo significant reorganization upon ligand binding.[82] The picosecond dynamics in 6C8 are likely to result from CDR3 amino acid side chain librations and entire loop motions, if the loops are sufficiently flexible. The length and composition of the 6C8 CDR3 loops suggest that they have different flexibilities. The LC CDR3 is eight residues long and contains no glycine residues, while the HC CDR3 is fourteen residues long and contains four glycine residues, of which two are consecutive. Thus, motions of the heavy-chain loop are expected to occur on a faster timescale than those of the light chain, and these heavy-chain motions may contribute to the picosecond timescale motions observed in the 3PEPS experiment. This model of protein motion is currently being tested by 3PEPS characterization of mutant proteins.

Characterization of the three anti-Fl Ab, 33F10, 40G4, and 4-4-20, showed that they respond to Ag excitation with an ultrafast motion ($<$ 40 fs), as well as slower 3 – 5-ps and over 3-ns timescale motions.[98] However, a comparison of the $\rho(\omega)$ values for each Ab (Figure 6) shows that there are significant differences in the amplitudes of these motions, which indicates distinctly different flexibilities. The largest differences are seen for the highest frequency (fastest timescale) motion. The fast motions within the 34F10 combining site are the most capable of

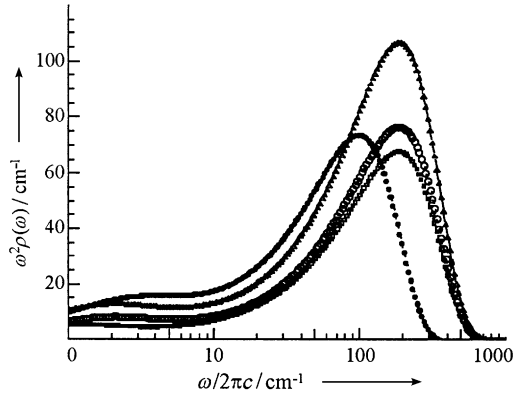

Figure 6. *Model spectral densities ρAb(ω) for Fl in Ab 34F10 (triangles), 40G4 (open circles), and 4-4-20 (squares), and MPTS in Ab 6C8 (solid circles).*

accommodating electronic and geometrical changes in Fl. The fastest motions of Ab 4-4-20 are the least able to respond to changes in Fl. The picosecond- and nanosecond-timescale motions of the anti-Fl Ab show decreasing flexibility upon proceeding from 34F10 to 40G4 to 4-4-20.

A high-resolution crystal structure is available for the Ab 4-4-20 – Fl complex.[100, 101] Along with calculations that predict how Fl changes upon excitation, the structure may be used to identify the parts of Ab 4-4-20 that may be most affected by the induced force (Figure 7). Calculations predict that the most significant

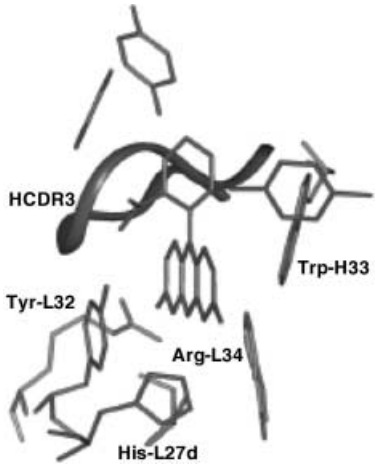

Figure 7. *Fl binding site in Ab 4-4-20 taken from the X-ray structure (Protein Data Bank code 1FLR).*

structural change associated with Fl excitation is rotation about the interannular bond connecting the xanthene ring to the carboxyphenyl ring. Most of the binding interactions are between the Ab and the xanthene ring of Fl,[97] with the carboxyphenyl ring hydrogen bonded to TyrL32 and packed from one side by HC CDR3 loop backbone atoms. These arguments, in addition to the relative reduced masses of the two rings predict that the force applied to the Ab will be manifest on residues of the HC CDR3 and TyrL32.

Calculations also predict significant charge redistribution, which is expected to cause changes in hydrogen bonding. In particular, these calculations predict a significant migration of charge away from both oxygen atoms of the xanthene ring upon excitation. As a result, hydrogen bonds observed in the crystal structure between these atoms and HisL27D and ArgL34 will be weakened upon Ag excitation. Motion of these side chains, after their release from strong hydrogen bonds, may also contribute to the observed motions. Thus, the observed protein response in 4-4-20 is likely to result from motions of residues of the HC CDR3 loop, TyrL32, HisL27D, and ArgL34.

In light of these structural arguments, it is interesting to speculate on the observed rigidity of the 4-4-20 complex with Fl, relative to the two other Ab – Fl complexes. Interestingly, the length of the HC CDR3 loop parallels the observed flexibilities: the loop length of the most flexible Ab, 34F10, is 12 amino acids; the second most flexible, 40G4, is 10 amino acids long; and the most rigid Ab, 4-4-20, is 7 amino acids long. This parallel supports the rather intuitive notion that longer loops may impart combining sites with increased flexibility, as suggested above. An additional unique feature of the 4-4-20 complex may contribute to its rigidity. TyrL32 hydrogen bonds with the phenylcarboxylate moiety and also packs on the xanthene ring. This side chain may act as a 'molecular splint' that bridges the highly flexible interannular bond, and may therefore be particularly sensitive to the relative geometry of the two rings. TyrL32 is unique to 4-4-20 as it is part of an insertion within the 4-4-20 LC CDR1 that is not present in either 34F10 or 40G4. This molecular interpretation supports a contribution of induced fit to the 4-4-20 interaction with Fl.

The murine immune system responds to MPTS and Fl by evolving different combining sites with distinct dynamics. Three timescales of protein motion are observed for both 6C8 and the anti-Fl Ab. The two fastest timescales, under 100 fs and 1 – 3 ps, are similar in all Ab. However, 6C8 shows 67-ps dynamics that are not present in the anti-Fl Ab. Moreover, the slowest protein motions in the anti-Fl Ab are significantly slower than those in 6C8, which indicates that the anti-Fl Ab are generally more flexible than the Ab that binds MPTS. Even though the induced displacements are smaller with MPTS than with Fl, these displacements are resisted by higher frequency protein motions, resulting in larger reorganization energies. The more flexible Ag (Fl) appears to have selected more flexible Ab (4-4-20, 34F10, and 40G4), while the more rigid Ag (MPTS) appears to have selected a more rigid Ab (6C8). This may imply that the mechanism of recognition, lock-and-key, induced fit, or conformational selection, may be optimal when reflected in both binding partners, and that flexible proteins are evolved to bind flexible targets, whilst rigid proteins are evolved to bind rigid targets.

5. Outlook

Relative to their abiological counterparts, biological macromolecules are unique in terms of their complexity and the fact that they have been built by evolution. The connection to evolution is a central component of dynamic theories that emphasize molecular motions in addition to ground state and transition state stability arguments. The experimental approaches described above, driven not only by physical methods, but also by synthetic organic chemistry and molecular biology, have the potential to test the different models of biomolecular dynamics. The data thus far, for example, the effect of the DNA duplex environment on tautomerization, the relationship of protein flexibility to redox activity in cyt *c*, and the response of an Ab to an applied force, are all consistent with the conventional thermodynamic view. However, it is certainly too early to make generalizations. We are beginning to apply the techniques to enzymes, which are perhaps the biomolecules most likely to show important dynamic behavior.

[1] M. J. Knapp, J. P. Klinman, *Eur. J. Biochem.* **2002**, *269*, 3113 – 3121.
[2] M. J. Sutcliffe, N. S. Scrutton, *Eur. J. Biochem.* **2002**, *269*, 3096 – 3102.
[3] R. C. Noonan, C. W. Carter, C. K. Bagdassarian, *Protein Sci.* **2002**, *11*, 1424 – 1434.
[4] T. C. Bruice, S. J. Benkovic, *Biochemistry* **2000**, *39*, 6267 – 6274.

[5] A. Warshel, *Acc. Chem. Res.* **2002**, *35,* 385 – 395.
[6] J. Villa, A. Warshel, *J. Phys. Chem. B* **2001**, *105*, 7887 – 7907.
[7] A. Warshel, W. W. Parson, *Q. Rev. Biophys.* **2001**, *34*, 563 – 679.
[8] D. Antoniou, S. Caratzoulas, C. Kalyanaraman, J. S. Mincer, S. D. Schwartz, *Eur. J. Biochem.* **2002**, *269*, 3103 – 3112.
[9] J. L. Radkiewicz, C. L. Brooks, *J. Am. Chem. Soc.* **2000**, *122*, 225 – 231.
[10] M. Chachisvilis, T. Fiebig, A. Douhal, A. H. Zewail, *J. Phys. Chem. A* **1998**, *102*, 669 – 673.
[11] A. Douhal, S. K. Kim, A. H. Zewail, *Nature* **1995**, *378*, 260 – 263.
[12] A. Douhal, F. Lahmani, A. H. Zewail, *Chem. Phys.* **1996**, *207*, 477 – 498.
[13] D. E. Folmer, L. Roth, E. S. Wisniewski, A. W. Castleman, *Chem. Phys. Lett.* **1998**, *287*, 1 – 7.
[14] Y. Chen, F. Gai, J. W. Petrich, *Chem. Phys. Lett.* **1994**, *222*, 329 – 334.
[15] P.-T. Chou, C.-Y. Wei, G.-R. Wu, W.-S. Chen, *J. Am. Chem. Soc.* **1999**, *121*, 12186 – 12187.
[16] A. K. Ogawa, O. K. Abou – Zied, V. Tsui, D. A. C. R. Jimenez, F. E. Romesberg, *J. Am. Chem. Soc.* **2000**, *122*, 9917 – 9920.
[17] O. K. Abou – Zied, R. Jimenez, F. E. Romesberg, *J. Am. Chem. Soc.* **2001**, *123*, 4613 – 4614.
[18] O. K. Abou – Zied, R. Jimenez, E. H. Z. Thompson, D. P. Millar, F. E. Romesberg, *J. Phys. Chem. A* **2002**, *106*, 3665 – 3672.
[19] H. Wang, H. Zhang, O. K. Abou – Zied, C. Yu, F. E. Romesberg, M. Glasbeek, *Chem. Phys. Lett.* **2003**, *367 (5 – 6)*, 599 – 608.
[20] Y. Chen, F. Gai, J. W. Petrich, *J. Am. Chem. Soc.* **1993**, *115*, 10158 – 10166.
[21] G. J. Woolfe, M. Melzig, S. Schneider, F. Dorr, *Chem. Phys.* **1983**, *77*, 213 – 221.
[22] M. Krishnamurthy, S. K. Dogra, *J. Photochem.* **1986**, *32*, 235.
[23] T. Arthen – Engeland, T. Bultmann, N. P. Ernsting, M. A. Rodriguez, W. Thiel, *Chem. Phys.* **1992**, *163*, 43 – 53.
[24] M. A. Rios, M. C. Rios, *J. Phys. Chem.* **1995**, *99*, 12456 – 12460.
[25] M. Mosquera, J. C. Penedo, M. C. R. Rodriguez, F. Rodriguez – Prieto, *J. Phys. Chem.* **1996**, *100*, 5398 – 5407.
[26] K. J. Halverson, I. Sucholeiki, T. T. Ashburn, P. T. J. Lansbury, *J. Am. Chem. Soc.* **1991**, *113*, 6701 – 6703.
[27] L. Tadesse, R. Nazarbaghi, L. Walters, *J. Am. Chem. Soc.* **1991**, *113*, 7036 – 7037.
[28] A. Barth, C. Zscherp, *Q. Rev. Biophys.* **2002**, *35*, 369 – 430.
[29] J. W. Brauner, C. Dugan, R. Mendelsohn, *J. Am. Chem. Soc.* **2000**, *122*, 677 – 683.
[30] P. Hamm, M. Lim, W. F. DeGrado, R. M. Hochstrasser, *Proc. Natl. Acad. Sci. U.S.A.* **1999**, *96*, 2036 – 2041.
[31] S. M. Decatur, J. Antonic, *J. Am. Chem. Soc.* **1999**, *121*, 11914 – 11915.
[32] R. A. Gangani, D. Silva, J. Y. Nguyen, S. M. Decatur, *Biochemistry* **2002**, *41*, 15296 – 15303.
[33] H. Deng, R. Callender, *Methods Enzymol.* **1999**, *308*, 176 – 201.
[34] J. O. Alben, W. S. Caughey, *Biochem.* **1968**, *7*, 175 – 183.
[35] J. G. Belasco, J. R. Knowles, *Biochemistry* **1980**, *5*, 472 – 477.
[36] J. Fisher, J. G. Belasco, S. Khosla, J. R. Knowles, *Biochemistry* **1980**, *19*, 2895 – 2901.
[37] C. W. Wharton, *Nat. Prod. Rep.* **2000**, *17*, 447 – 453.
[38] V. Cepus, A. J. Scheidig, R. S. Goody, K. Gerwert, *Biochemistry* **1998**, *37*, 10263 – 10271.
[39] J. H. Wang, D. G. Xiao, H. Deng, M. R. Webb, R. Callender, *Biochemistry* **1998**, *37*, 11106 – 11116.
[40] P. Hellwig, T. Mogi, F. L. Tomson, R. B. Gennis, J. Iwata, H. Miyoshi, W. Mantele, *Biochemistry* **1999**, *38*, 14683 – 14689.
[41] A. Barth, W. Mantele, *Biophys. J.* **1998**, *75*, 538 – 544.
[42] M. Lim, T. A. Jackson, P. A. Anfinrud, *J. Chem. Phys.* **1995**, *102*, 4355 – 4366.
[43] J. R. Hill, D. D. Dlott, C. W. Rella, K. A. Peterson, S. M. Decatur, S. G. Boxer, M. D. Fayer, *J. Phys. Chem.* **1996**, *100*, 12100 – 12107.
[44] K. D. Rector, J. R. Engholm, J. R. Hill, D. J. Myers, R. Hu, S. G. Boxer, D. D. Dlott, M. D. Fayer, *J. Phys. Chem. B* **1998**, *102*, 331 – 333.
[45] G. N. J. Phillips, M. L. Teodoro, T. Li, B. Smith, J. S. Olsen, *J. Phys. Chem. B* **1999**, *103*, 8817 – 8829.
[46] K. D. Rector, C. W. Rella, J. R. Hill, A. S. Kwok, S. G. Sligar, E. Y. T. Chien, D. D. Dlott, M. D Fayer, *J. Phys. Chem. B* **1997**, *101*, 1468 – 1475.
[47] M. Lim, T. A. Jackson, P. A. Anfinrud, *Science* **1995**, *269*, 962 – 966.
[48] P. A. Anfinrud, C. Han, R. M. Hochstrasser, *Proc. Natl. Acad. Sci. U.S.A.* **1989**, *86*, 8387 – 8391.
[49] T. Lian, B. Locke, Y. Kholodenko, R. M. Hochstrasser, *J. Phys. Chem.* **1994**, *98*, 11648 – 11656.
[50] J. P. M. Schelvis, Y. Zhao, M. A. Marletta, G. T. Babcock, *Biochemistry* **1998**, *37*, 16289 – 16297.
[51] C. Varotsis, M. Vamvouka, *J. Phys. Chem. B* **1999**, *103*, 3942 – 3946.
[52] E. B. J. Wilson, J. C. Decius, P. C. Cross, *Molecular Vibrations*, Dover Publications, New York, **1955**.
[53] S. Masatoki, K. Ohno, H. Yoshida, H. Matsuura, *J. Phys. Chem.* **1996**, *100*, 8487 – 8498.
[54] L. Grajcar, M. H. Baron, S. Becourarn, S. Czernecki, J. M. Vallery, C. Reiss, *Spectrochim. Acta Part A* **1994**, *50*, 1015 – 1022.
[55] K. Ohno, H. Abe, S. Masatoki, H. Yoshida, H. Matsuura, *J. Phys. Chem.* **1996**, *100*, 12674 – 12679.
[56] K. Ohno, S.-i. Nomura, H. Yoshida, H. Matsuura, *Spectrochim. Acta Part A* **1999**, *55*, 2231 – 2246.
[57] K. Ohno, Y. Takagi, H. Matsuura, *J. Phys. Chem.* **1993**, *97*, 5530 – 5534.
[58] K. Ohno, H. Yoshida, H. Matsuura, *Spectrochim. Acta Part A* **1996**, *52*, 1377 – 1389.
[59] R. A. Dluhy, R. Mendelsohn, H. L. Casal, H. H. Mantsch, *Biochemistry* **1983**, *22*, 1170 – 1177.
[60] I. Echabe, M. A. Requero, F. M. Goñi, J. L. R. Arrondo, A. Alonso, *Eur. J. Biochem.* **1995**, *231*, 199 – 203.
[61] B. Pastrana, A. J. Mautone, R. Mendelsohn, *Biochemistry* **1991**, *30*, 10058 – 10064.
[62] S. C. Hsi, A. P. Tulloch, H. H. Mantsch, D. G. Cameron, *Chem. Phys. Lipids* **1982**, *31*, 97 – 103.
[63] J. Jortner, R. D. Levine, B. Pullman, *Twenty-fourth Jerusalem Symposium on Quantum Chemistry and Biochemistry* (Jerusalem, Israel), Mode Selective Chemistry, **1991**.
[64] J. K. Chin, R. Jimenez, F. E. Romesberg, *J. Am. Chem. Soc.* **2002**, *124*, 1846 – 1847.
[65] J. K. Chin, R. Jimenez, F. E. Romesberg, *J. Am. Chem. Soc.* **2001**, *123*, 2426 – 2427.
[66] M. Laberge, J. M. Vanderkooi, K. A. Sharp, *J. Phys. Chem.* **1996**, *100*, 10793 – 10801.
[67] T. P. Lo, J. G. Guillemette, G. V. Louie, M. Smith, G. D. Brayer, *Biochemistry* **1997**, *34*, 163 – 171.
[68] G. D. Brayer, M. E. P. Murphy, *Cytochrome c: A Multidisciplinary Approach, Vol. 103*, University Science Books, Sausalito, **1995**.
[69] S. E. Hilgen, G. J. Pielak, *Protein Eng.* **1991**, *4*, 575 – 578.
[70] L. Banci, I. Bertini, H. B. Gray, C. Luchinat, T. Reddig, A. Rosato, P. Turano, *Biochemistry* **1997**, *36*, 9867 – 9877.
[71] R. A. Scott, A. G. Mauk, *Cytochrome c: A Multidisciplinary Approach*, University Science Books, Sausalito, **1995**.
[72] F. A. Tezcan, J. R. Winkler, H. B. Gray, *J. Am. Chem. Soc.* **1998**, *120*, 13383 – 13388.
[73] A. K. Churg, A. Warshel, *Biochemistry* **1986**, *25*, 1675 – 1681.
[74] D. H. Murgida, P. Hildebrandt, *J. Am. Chem. Soc.* **2001**, *123*, 4062 – 4068.
[75] C. Blouin, C. J. A. Wallace, *J. Biol. Chem.* **2001**, *276*, 28814 – 28818.
[76] I. Muegge, P. X. Qi, A. J. Wand, Z. T. Chu, A. Warshel, *J. Phys. Chem. B.* **1997**, *101*, 825 – 836.
[77] Unpublished result.
[78] L. Pauling, *Chem. Eng. News* **1946**, *24*, 1375 – 1377.
[79] D. E. Koshland, *Proc. Natl. Acad. Sci. U.S.A.* **1958**, *44*, 98 – 104.
[80] I. A. Wilson, R. L. Stanfield, *Curr. Opin. Struct. Biol.* **1994**, *4*, 857 – 867.
[81] P. A. Patten, N. S. Gray, P. L. Yang, C. B. Marks, G. J. Wedemayer, J. J. Boniface, R. C. Stevens, P. G. Schultz, *Science* **1996**, *271*, 1086 – 1091.
[82] J. M. Rini, U. Schulze-Gahmen, I. A. Wilson, *Science* **1992**, *255*, 959 – 965.
[83] U. Schulze – Gahmen, J. M. Rini, I. A. Wilson, *J. Mol. Biol.* **1993**, *234*, 1098 – 1118.
[84] T. Scherf, R. Hiller, J. Anglister, *FASEB J.* **1995**, *9*, 120 – 126.
[85] J. N. Herron, X. M. He, D. W. Ballard, P. R. Blier, P. E. Pace, A. L. Bothwell, E. W. Voss, A. B. Edmundson, *Proteins* **1991**, *11*, 159 – 175.
[86] J. Tormo, D. Blaas, N. R. Parry, D. Rowlands, D. Stuart, I. Fita, *EMBO J.* **1994**, *13*, 2247 – 2256.
[87] T. Bizebard, B. Gigant, P. Rigolet, B. Rasmussen, O. Diat, P. Bosecke, S. A. Wharton, J. J. Skehel, M. Knossow, *Nature* **1995**, *376*, 92 – 94.
[88] J. Lescar, R. Stouracova, M.-M. Riottot, V. Chitarra, J. Brynda, M. Fabry, M. Horeisi, J. Sedlacek, G. A. Bentley, *J. Mol. Biol.* **1997**, *267*, 1207 – 1222.
[89] F. E. Romesberg, B. Spiller, P. G. Schultz, R. C. Stevens, *Science* **1998**, *279*, 1929 – 1933.
[90] J. Foote, C. Milstein, *Proc. Natl. Acad. Sci. U.S.A.* **1994**, *91*, 10370 – 10374.
[91] L. C. James, P. Roversi, D. S. Tawfik, *Science* **2003**, *299*, 1362 – 1367.

[92] M. D. Fayer, *Annu. Rev. Phys. Chem.* **2001**, *52*, 315 – 356.
[93] C. W. Rella, A. Kwok, K. Rector, J. R. Hill, H. A. Schwettman, D. D. Dlott, M. D. Fayer, *Phys. Rev. Lett.* **1996**, *77*, 1648 – 1651.
[94] M. Lim, P. Hamm, R. M. Hochstrasser, *Proc. Natl. Acad. Sci. U.S.A.* **1998**, *95*, 15315 – 15320.
[95] G. R. Fleming, M. Cho, *Annu. Rev. Phys. Chem.* **1996**, *47*, 109 – 134.
[96] S. Mukamel, *Principles of Nonlinear Optical Spectroscopy*, Oxford University Press, New York, **1995**.
[97] R. Jimenez, D. A. Case, F. E. Romesberg, *J. Phys. Chem. B* **2002**, *106*, 1090 – 1103.
[98] R. Jimenez, G. Salazar, K. K. Baldridge, F. E. Romesberg, *Proc. Natl. Acad. Sci. U.S.A.* **2003**, *100*, 92 – 97.
[99] Single residues in the light and heavy chains are denoted by the three-letter amino acid code, the letter 'L' or 'H' to denote the chain, and the residue number.
[100] J. N. Herron, A. H. Terry, S. Johnston, X.-M. He, L. W. Guddat, E. W. Voss, A. B. Edmundson, *Biophys. J.* **1994**, *67*, 2167 – 2183.
[101] M. Whitlow, A. J. Howard, J. F. Wood, E. W. Voss, K. D. Hardman, *Protein Eng.* **1995**, *8*, 749 – 761.

Received: February 6, 2003 [M572]

